Chilling and forcing temperatures interact to predict the onset of wood formation in Northern Hemisphere conifers

Nicolas Delpierre, Ségolène Lireux, Florian Hartig, Jesus Julio Camarero, Alissar Cheaïb, Henri Cuny, Annie Deslauriers, Patrick Fonti, Jozica Gricar, Jian-Guo Huang, et al.

DR. NICOLAS DELPIERRE (Orcid ID : 0000-0003-0906-9402)

DR. JESUS JULIO CAMARERO (Orcid ID : 0000-0003-2436-2922)

DR. JIAN-GUO HUANG (Orcid ID : 0000-0003-3830-0415)

MS. GUOHUA LIU (Orcid ID : 0000-0003-3164-3829)

DR. HARRI MÄKINEN (Orcid ID : 0000-0002-1820-6264)

DR. PETER PRISLAN (Orcid ID : 0000-0002-3932-6388)

Article type : Primary Research Articles

Chilling and forcing temperatures interact to predict the onset of wood formation in Northern Hemisphere conifers.

Running head: Temperature dependence of spring xylem onset

Nicolas Delpierre[1,*], Ségolène Lireux[1], Florian Hartig[2], J. Julio Camarero[3], Alissar Cheaib[1,4], Katarina Čufar[5], Henri Cuny[6], Annie Deslauriers[7], Patrick Fonti[8], Jožica Gričar[9], Jian-Guo Huang[10], Cornelia Krause[7], Guohua Liu[1,11], Martin de Luis[12], Harri Mäkinen[13], Edurne Martinez del Castillo[12], Hubert Morin[7], Pekka Nöjd[13], Walter Oberhuber[14], Peter Prislan[9],

Sergio Rossi[7,10], Seyedehmasoumeh Saderi[15], Vaclav Treml[16], Hanus Vavrick[17], Cyrille B. K. Rathgeber[15]

[1] Ecologie Systématique Evolution, Univ. Paris-Sud, CNRS, AgroParisTech, Université Paris-Saclay, 91400 Orsay, France

[2] Theoretical Ecology, University of Regensburg, Universitätsstraße 31, 93053 Regensburg, Germany

[3] Instituto Pirenaico de Ecología, CSIC (IPE-CSIC), Avda. Montañana 1005, 50192 Zaragoza, Spain

[4] Département des Sciences de la Vie et de la Terre, Faculté des Sciences – Section IV, Université libanaise Hoch Al Oumara, 1801 Zahlé, Liban

[5] University of Ljubljana, Biotechnical Faculty, Jamnikarjeva 101, SI-1000 Ljubljana, Slovenia

[6] Institut National de l'Information Géographique et Forestière (IGN), 1 rue des blanches terres, 54250 Champigneulles, France

[7] Département des Sciences Fondamentales, Université du Québec à Chicoutimi, 555 boulevard de l'Université, Chicoutimi (QC), Canada

[8] Swiss Federal Research Institute WSL, Zuercherstrasse 111, 8903 Birmensdorf, Switzerland

[9] Slovenian Forestry Institute, Večna pot 2, SI-1000 Ljubljana, Slovenia

[10] Key Laboratory of Vegetation Restoration and Management of Degraded Ecosystems of the Chinese Academy of Sciences, Guangdong Provincial Key Laboratory of Applied Botany, South China Botanical Garden of the Chinese Academy of Sciences, Guangzhou 510650, China

[11]College of Urban and Environmental Sciences, Laboratory for Earth Surface Processes of the Ministry of Education, Peking University, Beijing, China

[12] University of Zaragoza, Department of Geography and Regional Planning, C/Pedro Cerbuna 12, Zaragoza, 50009, Spain

[13] Natural Resources Institute Finland, Tietotie 2, 02150 Espoo, Finland

[14] Department of Botany, University of Innsbruck, 6020 Innsbruck, Austria

[15] Université de Lorraine, AgroParisTech, INRA, Silva, F-54000 Nancy, France

[16] Department of Physical Geography and Geoecology, Faculty of Science, Charles University, Albertov 6, 128 43 Prague, Czech Republic

[17] Department of Wood Science, Faculty of Forestry and Wood Technology, Mendel University in Brno,
Zemědělská 3, 613 00 Brno, Czech Republic

* author for correspondence : nicolas.delpierre@u-psud.fr ; Tel: 0033+(0)1 69 15 56 77;
ORCID : 0000-0003-0906-9402

Abstract

The phenology of wood formation is a critical process to consider for predicting how trees from the temperate and boreal zones may react to climate change. Compared to leaf phenology, however, the determinism of wood phenology is still poorly known. Here, we compared for the first time three alternative ecophysiological model classes (*threshold* models, *heat-sum* models and *chilling-influenced heat-sum* models) and an empirical model in their ability to predict the starting date of xylem cell enlargement in spring, for four major Northern Hemisphere conifers (*Larix decidua*, *Pinus sylvestris*, *Picea abies* and *Picea mariana*). We fitted models with Bayesian inference to wood phenological data collected for 220 site-years over Europe and Canada. The chilling-influenced heat-sum model received most support for all the four studied species, predicting validation data with a 7.7-day error, which is within one-day of the observed data resolution. We conclude that both chilling and forcing temperatures determine the onset of wood formation in Northern Hemisphere conifers. Importantly, the chilling-influenced heat-sum model showed virtually no spatial bias whichever the species, despite the large environmental gradients considered. This suggests that the spring onset of wood formation is far less affected by local adaptation than by environmentally-driven plasticity. In a context of climate change, we therefore expect rising winter-spring temperature to exert ambivalent effects on the spring onset of wood formation, tending to hasten it through the accumulation of forcing temperature, but imposing a higher forcing-temperature requirement through the lower accumulation of chilling.

Keywords: wood phenology, cambium, phenological models, chilling temperatures, forcing temperatures, conifers.

Introduction

The seasonality of physiological processes is an essential component of terrestrial ecosystem models (TEMs; Delpierre et al., 2012; Kramer, 1995), but is usually poorly represented being mostly confined to the simulation of leaf onset and leaf loss (Delpierre, Vitasse, et al., 2016). In such models, the phenology of non-leaf organs or tissues (e.g. wood) is simulated (i)

simultaneous or relative to leaf phenology or (ii) using generic, non-organ-specific temperature functions for modulating the allocation of carbon (Delpierre, Vitasse, et al., 2016 ; but see Schiestl-Aalto, Kulmala, Mäkinen, Nikinmaa, & Mäkelä, 2015). This reflects the state of our knowledge on the phenology of trees, which is far more developed for leaves as compared with other organs or tissues (Delpierre, Vitasse, et al., 2016; Ford, Harrington, Bansal, Gould, & St. Clair, 2016). It is difficult to quantify how strongly this knowledge gap affects the predictive ability of TEMs, but it certainly jeopardizes their biological realism (Guillemot et al., 2017). For example, it has been demonstrated in evergreen conifers that the spring resumption of cambium activity generally occurs before budburst (Cuny, Rathgeber, Lebourgeois, Fortin, & Fournier, 2012; Gruber, Strobl, Veit, & Oberhuber, 2010; Huang, Deslauriers, & Rossi, 2014; Michelot, Simard, Rathgeber, Dufrêne, & Damesin, 2012; Rossi et al., 2009). Moreover, several studies have shown that, independent from leaf phenology, the duration of the wood growing season *per se* is a major determinant of wood production (Delpierre, Berveiller, Granda, & Dufrêne, 2016; Lempereur et al., 2015), so that an earlier onset of cambium activity, or a later cessation may result in a higher cell production (Lupi, Morin, Deslauriers, & Rossi, 2010; Mäkinen, Jyske, & Nöjd, 2018). Consequently, there is a clear need for the development of wood phenology modules for inclusion into TEMs.

In order to develop wood phenology modules for TEMs, we first have to understand the causal climatic drivers of wood phenology. In the temperate and boreal regions of the Northern Hemisphere, the formation of wood is seasonal and occurs from late spring to early autumn (Rossi et al., 2016, 2008). In spring, cambial mother cells start dividing, producing new derivatives of phloem outward and xylem inward (Larson, 1994; Vaganov, Hughes, & Shashkin, 2006). As a base model for this cycle, several authors have proposed that, just as for buds, the spring resumption of cambium activity is the outcome of a two-phase dormancy period (Begum et al., 2018; Begum, Nakaba, Yamagishi, Oribe, & Funada, 2013; Ford et al., 2016; Little & Bonga, 1974; Rensing & Samuels, 2004). According to this model, cambium activity is prevented by tree's *internal* factors (e.g. physiological state, signals) during the *endo*-dormancy phase; while it resumes during the *eco*-dormancy phase when the *external* conditions are favourable.

The main candidate for external conditions driving the resumption of cambium activity in temperate and boreal ecosystems is the spring temperature (as reviewed in Begum et al., 2018; Delpierre, Vitasse, et al., 2016; Larson, 1994). Field observation have shown that spring cambium resumption is usually delayed at high altitudes and latitudes as compared to low

altitudes and latitudes (Jyske, Mäkinen, Kalliokoski, & Nöjd, 2014; Moser et al., 2010; Rossi et al., 2016; Rossi, Deslauriers, Anfodillo, & Carraro, 2007; Rossi et al., 2008). Furthermore, local stem heating activated the formation of wood (Gričar et al., 2007), with a gradually increased response to heat applied from winter to spring (Oribe & Kubo, 1997).

Based on these evidences, previous studies have developed different model formulations based on spring temperature to predict the timing of cambial resumption. A first model class uses a *temperature threshold* for predicting the onset of cambial activity in conifers from cold biomes (Deslauriers, Rossi, Anfodillo, & Saracino, 2008; Rossi et al., 2007, 2008). However, although this model is able to identify likely periods of cambial activity, its accuracy for predicting the onset of cambial activity from temperature time series is probably low (Fig. S1). Another model class is that of *heat sums* (Giagli, Gricar, Vavrcik, & Gryc, 2016; Schmitt, Jalkanen, & Eckstein, 2004; Seo, Eckstein, Jalkanen, Rickebusch, & Schmitt, 2008; Swidrak, Gruber, Kofler, & Oberhuber, 2011). Their underlying hypothesis is that the cambium resumes its activity (cell division followed by cell differentiation) after sufficient exposure to temperatures above a threshold (so-called *forcing* temperatures). Thus, *heat sum* models mimic the progress of cambium through the eco-dormancy phase, making the implicit hypothesis that the endo- and eco-dormancy phases are sequential, and that endo-dormancy stops at the date when heat accumulation starts (Delpierre, Vitasse, et al., 2016). In practice, a degree-days accumulation is calculated by summing temperatures above a threshold ('base temperature') of typically +5°C (or more rarely lower values e.g. 0-1°C, see Antonucci et al., 2015; Li et al., 2017) from a given day, fixed a priori, before the onset date of cambial reactivation. However, there is no consensus concerning the day or period of year from which the cambium becomes sensitive to *forcing* temperatures. Some studies choose January 1 or spring equinox (Giagli et al., 2016; Schmitt et al., 2004), whereas others (Seo et al., 2008) consider the starting date occurring when trees have experienced a daily mean temperature above +5°C for at least five consecutive days. Moreover, *heat sum* models usually fail in identifying a species-specific heat sum threshold above which cambium would systematically be active (Giagli et al., 2016; Moser et al., 2010), which is indicative of their low structural realism and thus low predictive ability. More recently, *chilling-influenced heat sum* models have been shown able to predict spring cambial reactivation in Douglas fir (Ford et al., 2016). Similar to *heat sum* models, those models were originally designed for describing the progress of primary meristems (i.e. leaf or flower buds) from dormancy to budburst. Their basic hypothesis is that the cambium requires a lower accumulation of *forcing* temperatures during

the eco-dormancy phase when exposed to increasing levels of cold temperatures (so-called *chilling* temperatures, (Cannell & Smith, 1983; Little & Bonga, 1974) during the endo-dormancy phase, which may precede or be concomitant to the eco-dormancy phase (Chuine, Garcia de Cortazar-Atauri, Kramer, & Hänninen, 2013). The underlying physiological basis of such *chilling-influenced heat sum* models is not fully understood (Rinne et al., 2001; Singh, Svystun, AlDahmash, Jönsson, & Bhalerao, 2017). Last, a recent study made use of empirical models (linear regression of spring-averaged temperature) to predict the timing of cambial resumption (Rossi et al., 2016).

Though previous studies evaluated the ability of the three abovementioned model classes separately in simulating the date of the resumption of cambium activity in spring (threshold-type, Rossi, Morin, Deslauriers, & Plourde, 2011; *heat sums*, Seo et al., 2008; Swidrak et al., 2011; *chilling-influenced heat sums*, Ford et al., 2016; empirical regression, Rossi et al., 2016), there has been no comparison of those models merits on the same dataset. Here, we make use of a large number of field observation data collected over Europe and Canada (GLOBOXYLO database) to conduct for the first time a systematic evaluation of the causal factors affecting the breaking of cambial dormancy, and to propose an improved model of cambial spring resumption. Specifically, by identifying which model structure receives most support from observed data, we aim to evaluate: (1) if the resumption of cambium activity of Northern Hemisphere conifers in spring is more likely caused by the crossing of a given temperature threshold or by an accumulation of heat ("do *threshold* models outperform *heat sum* models?") and; (2) if observation data support the existence of a separate endo-dormancy phase that can be broken by chilling exposure ("do *chilling-influenced heat sum* models fit the data best?"). Our hypotheses are (1) *threshold* models are fine for identifying a thermal probability of cambium activity but have low predictive ability since the daily variability of temperature superimposed to seasonal variations cannot serve as a reliable cue for trees; (2) that over large geographical gradients, models incorporating both the effects of chilling and forcing temperature are better able to describe the variability in the beginning of wood formation (since over large climate zones, multiple climate limitations interact). Having identified the model structure best supported by the data, we then evaluate the biological reliability of its inferred parameters, for future use in Terrestrial Ecosystem Models.

Material and methods

Study sites

The selected study sites were extracted from the GLOBOXYLO database[a], a dataset gathering wood formation and meteorological information collected over the past 15 years from several research teams all over the world. The selected data concern the four most observed coniferous species (*Larix decidua* Mill. (LADE), *Pinus sylvestris* L. (PISY), *Picea abies* L. Karst. (PCAB) and *Picea mariana* (Mill.) BSP (PCMA)), covering a wide range of temperature and photoperiod conditions in the Northern Hemisphere (from 40.0°N to 67.5°N latitude, 79.2°W to 29.4°E longitude, and from 30 m to 2150 m altitudes) (Fig. 1, Table S1). Specifically, the dataset includes wood formation critical dates from 2001 to 2013 over 46 study sites for a total of 220 site-years, representing 1105 tree-site-year observations. All sampled trees were dominant individuals. The average (±SD) tree age was 124 ± 70 years, with a diameter at breast height (DBH) of 44 ± 30 cm, and a tree height of 21 ± 8 m (Table S1).

Wood formation data

Microcore sampling and preparation

At each study site, on average 5±2 trees were chosen and sampled weekly from March-April, depending on local climate conditions, to monitor wood formation. The collection, preparation, and analysis of wood samples followed a common protocol across sites. Wood microcores of 2 mm in diameter and 15-20 mm in length were collected weekly at breast height (1.3±0.3 m) over the growing season, using a Trephor® tool (Rossi, Anfodillo, & Menardi, 2006) or surgical bone sampling needles (Deslauriers, Morin, & Begin, 2003). Microcores were then cut with rotary or sledge microtomes in transverse sections of 10-30 µm thick, stained with safranine and astra blue or cresyl violet acetate and observed under bright-field and polarized light after coloration (Rossi, Deslauriers, & Anfodillo, 2006).

Determination of the spring resumption of xylem formation

We focus on the beginning of xylem cell enlargement (bE) as a critical, well-defined marker corresponding to the spring start-up of wood formation. Ultrastructural changes in cambial cells are the very first stage of growth reactivation. The bE occurs somewhat later than the onset of ultrastructural changes in cambial cells; but the latter is very difficult to observe

[a] https://www6.nancy.inra.fr/foret-bois-lerfob/Projets/Projets-en-cours/GLOBOXYLO

accurately and involves both xylem and phloem cells (Prislan, Čufar, Koch, Schmitt, & Gričar, 2013; Prislan, Schmitt, Koch, Gričar, & Čufar, 2011). It is therefore not often reported in wood formation monitoring studies. To quantify bE, the number of cells in each differentiation zone (cambial, enlargement, thickening, and mature) was counted along at least three radial files on the anatomical sections. Enlarging tracheids were characterized by radial diameter at least twice that of a cambial cell. We defined, at the tree level, the beginning of the enlargement phase (bE) as the date (day of year, DoY) when more than 50% of the observed radial files present at least one first enlarging tracheid (Rathgeber, Longuetaud, Mothe, Cuny, & Le Moguédec, 2011).

Temperature and photoperiod data

Mean daily temperatures have been collected at the study sites (Fig. 1). However, local weather stations were usually not installed before the start of the wood formation monitoring. To be able to consider in our models weather conditions also before the monitoring period, we used, for European sites, the WATCH gridded meteorological dataset (grid-resolution = 0.5°, Weedon et al., 2014) to extrapolate those missing data, after establishing linear regression between the local and corresponding WATCH temperature data (correlation between overlapping local and WATCH temperature time series was $0.95 < r < 0.99$), and removing the (low) biases of WATCH data. For Canadian sites, i.e. for *Picea mariana*, we did not extrapolate the temperature time series. Day length (the daily duration of the photoperiod) was calculated daily as a function of latitude, using astronomical formulae[b].

Models description

We compared three classes of ecophysiological models and one empirical model (Table 1) in their ability to predict the date of onset of xylem cell enlargement phase (bE) in the four tree species of interest. The three model classes are: (i) *threshold* models, (ii) *heat sum* models, (iii) *chilling-influenced heat sum* models. Since the patterns of xylem formation have been strongly related to mean temperatures over large geographical gradients (Rossi et al., 2016), we used an empirical model relating bE to early season (January-June) average temperature as a benchmark for ecophysiological models.

[b] See for example Pr Dennis Baldocchi's biometeorology course, lecture number 7 (https://nature.berkeley.edu/biometlab/index.php?scrn=espm129)

For all ecophysiological models, we used photoperiod thresholds to delineate the start and end of the endo- and eco-dormancy periods, different to most earlier phenological modelling studies, which usually considered temperature accumulation to start at a given day of year (e.g. usually January 1 in most phenological studies considering *heat sum* models; Linkosalo, Carter, Hakkinen, & Hari, 2000; Seo et al., 2008). This choice was motivated by the fact that our study covers a large latitudinal gradient over which a given calendar day (not perceptible by trees *per se*) may correspond to a large variations in photoperiod (a signal which is perceptible by trees).

Temperature- and photoperiod-threshold models

In this class of models, we assumed that bE occurs when a given temperature and/or photoperiod threshold has/have been crossed. A first formulation of this model (henceforth referred to as *Tt* model) is:

$$bE = \min(d) \ such\ that\ T(d) \geq T^* \ and\ d > -10 \qquad (1)$$

where *bE* is the beginning of the xylem enlargement period (DoY), *d* is a day of year (DoY), *T* is the daily average temperature, and *T** is a temperature threshold (°C). We assume that the passing of the temperature threshold necessarily occurs after winter solstice of the previous year (i.e. DoY 355 of the previous year, or DoY -10 of current year).

In case *bE* occurs when the thresholds of both temperature and photoperiod have been exceeded, the model (henceforth *TDLt* model) writes:

$$\begin{cases} bE = \min(\mathrm{d})\ such\ that\ \ T(d) \geq T^*\ and\ \ d > j \\ with\ j = \min(d)\ such\ that\ \ DL(d) \geq DL^*\ and\ d > -10 \end{cases} \qquad (2)$$

where *DL* is the daily photoperiod (hours) and *DL** is a photoperiod-threshold (hours).

Heat sum model

In the *heat sum* model, we assumed that bE occurs when a given accumulation of heat (above a temperature threshold, i.e. forcing temperatures) has been reached. The model (henceforth *HS* model) takes the form:

$$bE = \min(d) \ such\ that\ \ F(d) \geq F^* \qquad (3)$$

$$\text{with } \begin{cases} F(d) = \sum_{F_{start}}^{d} T_{diff}(d) \\ with\ T_{diff}(d) = \begin{cases} T(d) - T_f, & if\ T \geq T_f \\ 0, & if\ T \leq T_f \end{cases} \end{cases} \quad (4)$$

where T_f is a temperature-threshold above which forcing temperatures are accumulated, *F(d)* is the heat sum at day *d* (degree-days) and *F** is the forcing units requirement at which bE occurs (degree-days). In this model, the accumulation of forcing temperature starts at a given photoperiod threshold DL_{Fstart} (hours), occurring after the winter solstice of the previous year such that:

$$F_{start} = \min(d) \text{ such that } DL(d) \geq DL_{Fstart} \quad (5)$$

$$\text{with } d > -10$$

This model simulates the progress of cambium through the eco-dormancy phase and makes the implicit hypothesis that the preceding endo-dormancy phase ends on day F_{start}.

Chilling-influenced heat sum model

In the chilling-influenced heat sum model (*CiHS* model), the progress of cambium through the endo- and eco-dormancy phases is explicit, and bE occurs at the end of the eco-dormancy phase. During endo-dormancy, cambium division is inhibited by tree internal factors, the effects of which are counteracted by low temperatures. Following the approach proposed by (Cannell & Smith, 1983) for bud meristems, this hypothesis translates into an accumulation of chilling temperatures, quantified as a number of chilling units (C_{tot}, in chill units C.U.). C_{tot} is calculated on a daily basis from C_{start} (DoY), up to the C_{end} date as follows:

$$C_{tot}(d) = \sum_{C_{start}}^{C_{end}} R_c(T(d)) \quad (6)$$

where the daily rate of chilling (R_c) can be calculated as a linear function of temperature:

$$R_c(T(d)) = \begin{cases} 1\ if\ T(d) < T_c \\ 0\ if\ T(d) \geq T_c \end{cases} \quad (7)$$

where T_c is the temperature threshold (°C) below which chilling accumulation occurs.

Besides the accumulation of chilling, the model assumes that the progression of the cambium towards bE during eco-dormancy is favoured by the accumulation of forcing temperatures *F(d)*, as described in eq. 3-4. The *CiHS* model postulates that, as the accumulation of chilling

proceeds, the requirement for forcing temperatures decreases, such that the critical sum of forcing F^* is defined daily, and linearly depends on C_{tot}:

$$F^*(d) = g \times C_{tot}(d) + h \quad (8)$$

where g is the slope of the relation between required forcing units and chilling-accumulation (degree-days per C.U.), and h is the forcing units requirement in the absence of chilling (degree-days).

In this model, both the period of cambium sensitivity to chilling temperatures (delimited by days of year C_{start} and C_{end}, eq. 6) and the start of forcing temperature accumulation (on day of year F_{start}, eq. 4) are parameterized as photoperiods (through parameters DLC_{start}, DLC_{end} and DLF_{start}, respectively; see eq. 5 for the correspondence of e.g. day of year F_{start} with photoperiod DL_{Fstart}). We set the parameter bounds such that DLC_{start} (DLC_{end}) cannot occur earlier than the autumn equinox (winter solstice) of previous year. Letting the model inference procedure free to find the most likely photoperiod limits for chilling and forcing accumulation within a large range (from autumn equinox of the previous year up to summer solstice of the current year), our model may represent several temporal combinations of the chilling and forcing temperature accumulation functions, corresponding to different hypotheses of the interplay between the endo- and eco-dormancy phases (i.e. sequential and parallel; see (Chuine et al., 2013).

Empirical relation with spring average temperature

This empirical model (analogous to Rossi et al., 2016) assumes that bE can be related to spring temperature via a linear regression, such that:

$$bE = m_{T_{spg}} \times T_{spg} + p_{T_{spg}}, \quad (9)$$

where T_{spg} is the average January-June temperature (°C) calculated for each site-year, and mT_{spg} and pT_{spg} are parameters of the regression line.

Parameter estimation and model comparison through Bayesian inference

To assess the models' abilities to simulate bE dates, we randomly split the bE data observed at the tree scale into calibration vs. validation subsets, with 70% of the data for calibration, and 30% for validation. We checked that the distribution of the random calibration and validation

bE subsets did not differ (Wilcoxon rank sum test, p>0.50). Since the model fitting ability and inferred parameters may depend on the calibration subset used, we repeated the calibration procedure 30 times, using different calibration vs. validation subset combinations. The model evaluation results we report concern validation data, unless indicated.

Model parameters were fitted via Bayesian inference (see, e.g. Gelman, Carlin, Stern, & Rubin, 2004, and Fu, Campioli, Van Oijen, Deckmyn, & Janssens, 2012, for application in phenological modelling). The Bayesian framework calculates a posterior estimate and uncertainty for the model parameters, based on a prior distribution and the likelihood, defined as the probability of obtaining the observed data, given the model assumptions with their respective parameters. We use a Gaussian likelihood for all models:

$$L(\theta) = \prod_{i=1,n} \frac{1}{\sigma\sqrt{2\pi}} exp\left[-\frac{1}{2}\left(\frac{P(\theta)_i - O_i}{\sigma}\right)^2\right], \quad \text{(eq. 10)}$$

where O_i is the observed bE date (DoY) for site-year-tree *i*; $P(\theta)_i$ is the bE date (DoY) predicted by the model at point θ in the parameter space, and σ is the standard deviation of the Gaussian distribution.

For all models considered, the fitted parameters included temperature and day length thresholds, for which natural extremes are given by the temperature and day length observed across the dataset. We therefore used uniform priors with these values as boundaries.

Posterior distributions were estimated with a differential evolution MCMC (DEzs, implemented in the 'BayesianTools' R package, (Hartig, Minnuno, & Paul, 2017)). For each model and species, we ran 200,000 MCMC iterations and confirmed convergence of the chain after burn-in using the Gelman-Rubin criterion (Gelman, Meng, & Stern, 1996), requiring the *psrf* value for all parameters to be smaller than 1.05.

As a criterion to compare the models, we used posterior model weights, related to the Bayes factor (BF; Kass & Raftery, 1995, based on the model fit on the validation data. Assuming an equal prior weight on all models, the posterior weight for each model (PMW) is given by:

$$PMW_i = \frac{\mathrm{ML}_i}{\sum_j \mathrm{ML}_j} \qquad \text{(eq. 11)},$$

where ML is the marginal likelihood of model *i* or *j*. The marginal likelihood is the likelihood of the model for a given dataset, averaged over the parameter uncertainty. In our case, we calculated the ML for the validation data, with parameter uncertainties derived from the

posterior estimated with the calibration data. This approach of calculating the ML on a model calibrated by a subset of the data circumvents the known problem of the BF to be highly dependent on parameter priors (see, e.g., O'Hagan, 1995; van Oijen et al., 2013). The PMW can be intuitively interpreted as the probability that the respective model is 'true'. In order to get a representative evaluation of the model abilities, we averaged PMW calculations across the 30 model-validation procedures.

Beside PMWs, we calculated for illustration the models' root mean square error of prediction (RMSE) and Akaike Information Criteria (AIC), at the mode of their posterior parameter distributions (MAP).

Quantifying bias in the model predictions

We quantified the bias in model predictions of validation data at the scales of the tree, the site-year, the site ("is the model able to represent the inter-site variability of bE?") and the year ("is the model able to represent the local annual anomaly of bE after removing the local bE average?"). Since there is no consensus in the statistical literature on how to evaluate model bias, we used two different methods. *Method 1*: We plotted and computed the coefficients of the linear ordinary least-squares regression of observed (y-axis) versus predicted (x-axis) data, as recommended by (Piñeiro, Perelman, Guerschman, & Paruelo, 2008), and tested the null hypothesis: "the slope of the linear regression equals one and the intercept equals zero" (Wald test) using the LinearHypothesis function from the 'car' R package (Fox & Weisberg, 2011). *Method 2*: we performed a major axis (type II) linear regression of predicted (y-axis) versus observed (x-axis) data, and checked if the 95%-confidence intervals of the slope and intercept included one and zero, respectively (Mesplé, Troussellier, Casellas, & Legendre, 1996).

Results

Wood phenological observations

The observed bE dates spanned 90 days, ranging from March 16 (DoY 75) for a PISY tree at the southernmost site from the database ('Moncayo' site, Spain) to July 2 (DoY 183) for a LADE tree located at 1900-m on an altitudinal gradient ('Lötschental site', Switzerland; Table 2). In this dataset, PISY was the earliest species to resume xylem cell enlargement in spring, showing ca. three-week earlier average bE than PCAB and 7-week earlier than PCMA and

LADE. The amplitude of bE dates spanned by each species varied from 49 days in PCMA to 101 days in PISY, consistent with the size of the climate space occupied by each species in the dataset (Fig. 2).

Performance of the models

Whatever the tree species, the chilling-influenced heat sum model (*CiHS*) was identified as the best-supported (most likely) model for predicting bE, displaying the highest posterior model weights over validation data with PMW_{valid} from 0.67 to 1.00 (average 0.90; Table 3). The *CiHS* model largely outperformed models belonging to the *threshold* (i.e. *Tt* and *TDLt* models) or the *heat sum* (*HS*) classes, which both showed nil PMW_{valid} (Table 3). The prediction error of *CiHS* was substantially lower than that of other models structures (e.g. validation RMSE of *CiHS* was on average 1.3 days lower as compared to the heat-sum model *HS*, 3.6 days lower as compared to the temperature-and-photoperiod threshold model (*TDLt*), 9.8 days lower as compare to the temperature-threshold model (*Tt*), Table 3). In PCMA, the empirical model predicting bE as a linear function of spring temperature (*MST*) received some support (PMW_{valid}=0.33), but substantially less than *CiHS* (PMW_{valid}=0.67). Beside its performance at the tree scale (Table 3), the *CiHS* model was also good at representing the variability of bE across site-years (Fig. 3), across sites (Suppl. Fig. S2), and across years (Suppl. Fig. S3). The *CiHS* model yielded unbiased predictions of the observations at all aggregation scales according to Method 1 for model bias testing (Table 4). Method 2 pointed more contrasted results: it confirmed the absence of bias at the scales of the site and of the site-year (except for LADE in the latter case; Table 4). However, it pointed biased results at the tree scale, and as regards annual anomalies (except for PCMA). In those cases, Method 2 returned that the *CiHS* overestimated early bE and underestimated late bE dates (i.e. slopes of the major axis regression of predicted versus observed dates were less than one).

Posterior parameter estimates for the *CiHS* model

Since the *CiHS* model predicted unknown data best, we looked at its posterior parameter estimates to evaluate their biological reliability. We first note that most parameters of the *CiHS* model could be estimated well (meaning that prior uncertainty was considerably reduced), and that the estimates were similar across the 30 calibration-validation splittings of

410 the data (Fig. 4, see Table S2 for parameter values at the mode of the merged 30 posterior
411 distributions).

412 In all species, chilling accumulation (DL_{Cstart}) started earlier than or close to vernal equinox
413 (corresponding to 12-hour photoperiod, Fig. 4, occurring on DoY 81, Fig. 5) and generally
414 lasted up to late dates (defined by DL_{Cend}), potentially up to the summer solstice when
415 applicable. Notable exceptions were high-latitude PISY and PCAB. In PCAB, the duration of
416 chilling accumulation was very short at high latitudes, virtually non-existent at low latitudes
417 (Fig. 5) and presented a maximum duration of ca. 15 days at intermediate latitudes (ca. 54°N)
418 due to latitudinal variations of the photoperiod course in spring.

419 Chilling accumulation resulted in an actual reduction of the forcing requirement for bE (all *g*
420 parameters were negative, Fig. 4), with a strong sensitivity to chilling exposure in LADE (-
421 14.9 degree-days / chill unit) and PCAB (-27.9 degree-days / chill unit). The upper
422 temperature threshold for chilling accumulation (T_c) ranged from -5.6°C in PCAB to +6.1°C
423 in PCMA (Fig. 4) with a median across species of +1.6°C. The lower temperature threshold
424 for forcing accumulation (T_f) ranged from -2.9°C in PCAB to +3.4°C in LADE (Fig. 4) with a
425 median across species of +0.15°C. The start of forcing accumulation (defined by DL_{Fstart})
426 looked bounded by vernal equinox (Fig. 5). It occurred later than the start of chilling
427 accumulation in both spruce species (PCAB and PCMA), but earlier than the start of chilling
428 accumulation in PISY and LADE (Fig. 5).

429

430 **Discussion**

431 The purpose of this study was to improve our understanding of the phenology of wood
432 formation, and in particular to unravel the causal triggers for the spring onset of xylem growth
433 in coniferous species. To this end, we evaluated the ability of three families of
434 ecophysiological models and one empirical model to predict the start of the enlargement
435 period of the xylem cells. Our results demonstrate that models based on temperature sums
436 perform better than those based on temperature- and photoperiod-thresholds do (Table 3).
437 Moreover, our results clearly support the chilling-influenced heat sum model (*CiHS*),
438 explicitly considering the processes of chilling and forcing temperature accumulation, for the
439 prediction of the spring onset of wood formation. Beside its high posterior probability
440 compared to the other models, the *CiHS* model also predicted the spring onset of xylem

441 formation with good accuracy. Its RMSE on the validation data, averaging 7.7 days (Table 3),
442 is close to the temporal resolution of micro-core sampling from the trees (i.e. 7 days), and
443 similar to the typical prediction accuracy of budburst (i.e. primary meristems), when deployed
444 over continental gradients (e.g. Basler, 2016). The clear support for a chilling-influenced heat
445 sum for the modelling of spring xylem phenology is different from what is reported in
446 budburst model comparisons. For the latter, heat sums and chilling-influenced heat sums do
447 not usually differ in their fit (Basler, 2016; Vitasse et al., 2011).

448 The identification of the *CiHS* model as receiving most support from the inference procedure
449 suggests that both forcing and chilling temperatures play a role in determining the spring
450 resumption date of xylem formation. To our knowledge, there is no *direct* evidence in the
451 literature of a modulation of the date of onset of xylem cell formation in trees exposed to
452 various chilling temperatures during winter and/or spring. Stem heating experiments showed
453 that an artificial resumption of cambial activity can be triggered during late winter, but not in
454 early winter (Begum, Nakaba, Oribe, Kubo, & Funada, 2010). This observation supports the
455 existence of an endo-dormancy phase, during which the cambium activity is repressed by
456 unknown tree internal factors (Delpierre, Vitasse, et al., 2016, but see Singh et al., 2017, for a
457 review of dormancy processes in primary meristems). However, it does not prove, nor does it
458 quantify the role of chilling temperatures in hastening the reactivation of xylem formation in
459 spring. Thus, there is a clear need for quantifying the actual role of chilling temperatures in
460 modulating the spring resumption of xylem formation, in line with pioneer works regarding
461 buds and seeds (see Sarvas, 1974, reviewed in Hänninen, 2016), which have recently been
462 actualized (e.g. Flynn & Wolkovich, 2018).

463 We delineated the time periods for the accumulation of chilling or forcing temperatures with
464 photoperiod limits, instead of day of year (DoY) as usually done in phenological modelling
465 (see e.g. Olsson and Jönsson, 2014; Basler 2016) for examples over large latitudinal
466 gradients). If the use of DoY is perfectly sound in local studies (i.e. for which the relation
467 between DoY and photoperiod is unequivocal), it is questionable in studies spanning
468 continental scales since plants sense time from variations in the photoperiodic signal. Across a
469 latitudinal gradient, a given photoperiod is reached at different DoYs (except the 12-hour
470 photoperiod occurring at spring equinox (March 20) across the entire gradient). This resulted
471 in large differences in our southern vs. northern study sites as regards the timing of the
472 chilling accumulation for PCAB and the duration of both chilling and forcing accumulation in
473 PISY (Fig. 5), two species spanning large latitudinal gradients in our dataset. Whether such

variations of the actual dates of cambium sensitivity to temperatures are realistic remains to be determined. This could experimentally be done by comparing the sensitivity of cambium to chilling in genetically identical plants placed in various photoperiod conditions, either in climate chambers (as done for budburst, e.g. Basler and Körner, 2014) or in natural conditions (e.g. International Phenological Gardens, Chmielewski & Rötzer, 2001).

In the *CiHS* model, the threshold temperatures promoting the progress of the eco-dormancy phase (forcing temperature threshold, T_f, ranging from -2.9°C to +3.4°C, Fig. 4) were comparable to values generally used in the modelling of budburst (typically 0°C or +5°C, Hänninen, 2016), based on experimental results (from -5°C to +1°C in, Heide, 1993). On the other hand, the values of threshold chilling temperatures (T_c) determined by the parameter inference procedure span a larger range (from -5.6°C to +6.1°C) and appear quite low in the cases of PCAB (-5.6°C) and LADE (-1.1°C) as compared to the values either determined experimentally in buds and seeds (for which Sarvas, 1974, reports -3°C as a lower limit for chilling effectiveness) or considered by expert judgment (0°C to +4.5°C in Coville, 1920; +2°C to +4°C for cambium in Little & Bonga, 1974) as effective for chilling.

From a larger perspective, the questions about the plausibility of parameter values we inferred are further linked with the range of environmental conditions in which the bE data were obtained. Indeed, inferring model parameters from data acquired from trees growing under natural conditions, inevitably exposed to multiple interacting environmental factors (think e.g. of the strong concurrent latitudinal temperature and photoperiod gradient), is not equivalent to inferring them from a controlled experiment where the environmental conditions can be at least partially be disentangled (Verdier et al., 2014), and their biological interpretability is necessarily less generic. However, we noticed that our species-specific parameterizations of the *CiHS* model were able to reproduce the locally observed between-species difference in bE at those sites where two species of interest co-occur (Fig. 6), giving credit to the overall plausibility of the inferred parameters.

In this study we used model formulations initially developed for simulating the occurrence of budburst, assuming similar environmental controls of the phenology of primary and secondary meristems (Delpierre, Vitasse, et al., 2016). Even for budburst, those models lack an indisputable biological support (Clark, Salk, Melillo, & Mohan, 2014; Delpierre, Vitasse, et al., 2016). New model formulations for the phenology of budburst appear in the literature from time to time, considering more complex interactions of chilling and forcing temperatures

in interaction with photoperiod (e.g. Blümel & Chmielewski, 2012; Caffarra, Donnelly, & Chuine, 2011). Similar to the necessary effort to calibrate and compare those continuous-state budburst models to continuous data (for instance by measuring the release of plasmodesmata closure by callose, which is an indicator of bud endo-dormancy, Singh et al., 2017), a biologically-undisputable modelling of spring cambial activity will require the evaluation of those models with continuous seasonal markers of cambial cells activity (i.e. cytoplasmic changes in cambial cells such as presence and form of microtubules, vacuoles, lipid droplets, plastids and other cell organelles; Begum et al., 2012; Chaffey & Barlow, 2002; Prislan et al., 2013; Rensing & Samuels, 2004), or metabolite content.

Even if the *CiHS* model has no clear mechanistic foundation, we remind that the exposure to chilling temperature promotes soluble sugars accumulation from starch conversion, especially sucrose (along with raffinose, stachyose and other metabolites; Sakai & Larcher, 1987; Strimbeck, Schaberg, Fossdal, Schröder, & Kjellsen, 2015) that remain high until spring de-hardening. Since cell production is limited by local sucrose availability (Deslauriers, Huang, Balducci, Beaulieu, & Rossi, 2016), we posit that exposure to chilling temperatures may constitute a local pool of sucrose readily available for cell production when temperatures become favourable for mitosis and/or cell expansion. In case of low chilling, this local sucrose pool would be low, and carbon-fueling for cell formation would rely more on the resumption of photosynthesis, which responds to forcing temperature accumulation (Mäkelä, Hari, Berninger, Hänninen, & Nikinmaa, 2004; Pelkonen & Hari, 1980). This mechanistic hypothesis is coherent with the general behaviour of the *CiHS* model (the required forcing accumulation decreases with increasing chilling exposure), and would explain why we infer in some species low temperature thresholds for chilling accumulation (-1.1°C in LADE, -5.6°C in PCAB). Indeed, the rate of starch to sugar conversion has been shown to be maximum at temperatures from -3°C to -5°C, and continued down to -15°C (in *Salix sachalinensis* twigs, Sakai, 1966).

Moreover, the successful use of model structures designed and used to predict budburst to simulate the resumption of cambial spring activity raises the question of the coordination and interaction of the phenologies of tree organs (Delpierre, Vitasse, et al., 2016). Phytohormones can play a significant role; with e.g. auxins produced in expanding buds influencing the rate of stem cambial divisions (see review of Sorce, Giovannelli, Sebastiani, & Anfodillo, 2013). Yet, the important role of auxin is also interconnected with cytokinin in the vascular cambium. Although auxin peak in the middle of cambium and cytokinin in the middle of

phloem, the latter acts as a positive regulator of cell division in the vascular cambium by increasing the number of cambial cell (Immanen et al., 2016) because of its crucial role on the cell division cycle (Schaller, Street, & Kieber, 2014). Thus, the resumption of xylem formation in spring is at least partially independent from auxin-producing buds, as clearly demonstrated in stem heating experiments (where xylem formation resumes artificially whereas buds remain dormant, Begum et al., 2010; Gricar et al., 2006; Oribe, Funada, & Kubo, 2003), and from the observed earlier timing of enlargement of new xylem cells, as compared to bud elongation in the evergreen coniferous trees studied here (*Picea abies*, *Pinus sylvestris*, *Picea mariana*; Antonucci et al., 2015; Cuny et al., 2012; Huang et al., 2014; Michelot et al., 2012). The presence of auxins in overwintering tissues (Egierszdorff, 1981), and of a local pool of sucrose (see above) may decouple the onset of cambium division and xylem enlargement from the timing of bud elongation, as observed from stem heating experiments; along with the presence of signal-transduction chains involving phytochromes (proteins acting as photoreceptors, i.e. able to sense modifications of the photoperiod) in the cambium (Petterle, Karlberg, & Bhalerao, 2013), this suggests that the cambium may well respond to variations of environmental conditions independently from buds. This hypothesis is supported by inter-annual variability in the delays between the spring phenophases of wood and leaves in both gymnosperms (Cuny et al., 2012) and angiosperms (Takahashi, Okada, & Nobuchi, 2013).

The chilling-influenced heat sum model produced mostly unbiased results when the data were aggregated at the site-year or at the site scale (Table 4), pointing to its overall accurate capacity of to simulate the spring resumption of xylem formation in coniferous species. Yet, one of our bias-detection methods (method 2) suggested that the model underestimated the range of tree individual bE (in all species, Table 4) and the annual bE anomalies (in 3 out of 4 species, Table 4, Fig. S3). Though our models rely on environmental (temperature and photoperiod) data collected at the tree population scale, we conducted the parameter inference with the most basic level of information available (i.e. at the individual tree level, see section 2.5). It is clear that part of the model bias that is detected at the individual scale is related to the model structural incapacity to simulate the variety of individual tree responses to the same environment that is observed in a tree population (Delpierre, Guillemot, Dufrêne, Cecchini, & Nicolas, 2017) and can actually be quite large (e.g. the within-population SD of observed bE dates for a given year is 5 days on average, Table 2). Bias in the predictions of annual bE anomalies may further originate from the simplicity of the model structure, which probably

does not represent the whole range of environmental interactions resulting in the spring onset of xylem formation.

A study aiming at simulating the date of budburst of *Betula pendula* and *Picea abies* individuals from central to Northern Europe (i.e. a bioclimatic scale comparable to the one considered in our work) reported a lower performance over validation data as compared to our results for bE (with prediction RMSE of 8.9 and 9.1 days, respectively for their best heat sum model), along with a non-homogeneous bias over the continent, suggesting a role for the local adaptation of trees phenological traits (Olsson & Jönsson, 2014). It is not clear whether the latitudinal bias observed in Olsson & Jönsson (2014) originates from local adaptation (that has been evidenced several times for budburst, see e.g. Chuine, Mignot, & Belmonte, 2000; Osada et al., 2018; Vitasse, Delzon, Bresson, Michalet, & Kremer, 2009; von Wuehlisch, Krusche, & Muhs, 1995) or is related to the uncertainty of budburst observations recorded through local phenological protocols. The data we use in our work are less prone to such problems since the observations were collected and processed according to a common protocol across the entire study zone (Rathgeber et al., 2011; Rossi et al., 2016). To this respect, we conclude from the absence of bias in the prediction of site average dates of bE (Table 4, Fig. S2) that local adaptation is, if any, of marginal influence in determining bE (Perrin, Rossi, & Isabel, 2017) as compared to the plasticity of bE driven by varying temperature and photoperiod conditions.

This study is the first comparative assessment of ecophysiological models aiming at simulating the spring resumption of xylem formation in trees. We demonstrated that chilling-influenced heat sum models are best supported by the data for the four coniferous species studied. Thus, analogous to what is commonly observed for buds, we state that winter-spring temperatures exert ambivalent effects on the spring onset of wood formation (bE) (i.e. on the one hand, warmer temperatures tend to hasten the occurrence of bE through the accumulation of *forcing* temperature, but on the other hand they are associated to less *chilling*, imposing a higher forcing-temperature sum to trigger wood formation). Previous results from (Rossi et al., 2011) suggested that spring warming would result in a continuous trend to earlier bE in the next decades. Our results question these predictions, since warming reduces the number of chilling days. This is probably the cause of the recently evidenced reduced sensitivity of spring leaf phenology to warm temperatures (Fu et al., 2015), which we also forecast to happen for wood formation (note that the length of wood phenology time series is much shorter than for bud phenology, so that this hypothesis remains to be tested).

Our work paves the way for the development of ecophysiological models simulating the whole phenological sequence of wood formation. We expect the *CiHS* model to be included as a component of schemes representing the whole seasonal cycle of wood formation, into which subsequent wood formation phases would partially depend on the occurrence of bE (Hänninen & Kramer, 2007; Lupi et al., 2010). Such a model is also urgently needed in ecosystem models of the carbon cycle (Delpierre, Vitasse, et al., 2016) which are undergoing core changes in their representation of wood growth (Guillemot et al., 2017; Schiestl-Aalto et al., 2015).

Acknowledgements

The dataset on wood phenology was generated by the GLOBOXYLO initiative (https://www6.nancy.inra.fr/foret-bois-lerfob_eng/Projects/Current/GLOBOXYLO), which was developed in the framework of the FPS COST Action STReESS (FP1106, http://streess-cost.eu/). The study profited from a Bayesian inference spring school organized by Cost Action FP1304 PROFOUND. N.D. acknowledges support from the GIP-ECOFOR (SACROBOQUE project, grant # 2016.013). C.B.K.R acknowledges support from the French Ministry of Ecology (project GICC GRAAL 10-MCGOT-GICC-8-CVS-139) and the French National Research Agency (through ANR-11-LABX-0002-01, Lab of Excellence ARBRE). P.F. acknowledges the Swiss National Science Foundation (projects INTEGRAL-121859 and LOTFOR-150205). This work was also supported by grants from the Academy of Finland (Nos. 115650, 124390), the European Social Fund, the state budget of the Czech Republic, Project Indicators of trees vitality Reg. No. CZ.1.07/2.3.00/20.0265, the Slovenian Research Agency (ARRS; programs P4-0015 and P4-0107), the 100 Talents Program of the Chinese Academy of Sciences (Grant No. Y421081001), National Natural Science Foundation of China (Grant No. 31570584), Consortium de Recherche sur la Forêt Boréale Commerciale, Fonds de Recherche sur la Nature et les Technologies du Québec, Forêt d'enseignement et de recherche Simoncouche, and Natural Sciences and Engineering Research Council of Canada. We thank Marc Stéphanon for providing the WATCH data. The authors have no conflict of interest to declare.

Authors' contributions

N.D. and C.B.K.R initiated the project. N.D. designed the study, performed the research and wrote the manuscript. F.H. advised on the Bayesian inference framework. N.D., S.L., C.B.K.R., F.H. and A.D. analysed results. J.J.C., H.C., K.C., A.D., P.F., J.G., J.-G.H., C.K., M.L., H.M., E.M.C., P.N., W.O., P.P., S.R., V.T., H.V. and C.B.K.R. collected xylem micro-cores and produced phenological data. C.B.K.R. compiled the phenological database. E.M.C. made Figure 1. All authors commented on the manuscript.

References

Antonucci, S., Rossi, S., Deslauriers, A., Lombardi, F., Marchetti, M., & Tognetti, R. (2015). Synchronisms and correlations of spring phenology between apical and lateral meristems in two boreal conifers. *Tree Physiology*, *35*(10), 1086–1094. https://doi.org/10.1093/treephys/tpv077

Basler, D. (2016). Evaluating phenological models for the prediction of leaf-out dates in six temperate tree species across central Europe. *Agricultural and Forest Meteorology*, *217*, 10–21. https://doi.org/10.1016/j.agrformet.2015.11.007

Basler, D., & Körner, C. (2014). Photoperiod and temperature responses of bud swelling and bud burst in four temperate forest tree species. *Tree Physiology*, *34*(4), 377–388. https://doi.org/10.1093/treephys/tpu021

Begum, S., Kudo, K., Rahman, M. H., Nakaba, S., Yamagishi, Y., Nabeshima, E., Nugroho, W.D., Oribe, Y., Kitin, P., Jin, H.-O., & Funada, R. (2018). Climate change and the regulation of wood formation in trees by temperature. *Trees - Structure and Function*, *32*(1), 3–15. https://doi.org/10.1007/s00468-017-1587-6

Begum, S., Nakaba, S., Oribe, Y., Kubo, T., & Funada, R. (2010). Cambial sensitivity to rising temperatures by natural condition and artificial heating from late winter to early spring in the evergreen conifer Cryptomeria japonica. *Trees*, *24*(1), 43–52. https://doi.org/10.1007/s00468-009-0377-1

Begum, S., Nakaba, S., Yamagishi, Y., Oribe, Y., & Funada, R. (2013). Regulation of cambial activity in relation to environmental conditions: understanding the role of temperature in wood formation of trees. *Physiologia Plantarum*, *147*(1), 46–54. https://doi.org/10.1111/j.1399-3054.2012.01663.x

Begum, S., Shibagaki, M., Furusawa, O., Nakaba, S., Yamagishi, Y., Yoshimoto, J., Jin, H.-O., Sano, Y., Funada, R. (2012). Cold stability of microtubules in wood-forming tissues of conifers during seasons of active and dormant cambium. *Planta*, *235*(1), 165–179. https://doi.org/10.1007/s00425-011-1500-2

Blümel, K., & Chmielewski, F. M. (2012). Shortcomings of classical phenological forcing models and a way to overcome them. *Agricultural and Forest Meteorology*, *164*, 10–19. https://doi.org/10.1016/j.agrformet.2012.05.001

Caffarra, A., Donnelly, A., & Chuine, I. (2011). Modelling the timing of Betula pubescens budburst. II. Integrating complex effects of photoperiod into process-based models. *Climate Research*, *46*(2), 159–170. https://doi.org/10.3354/cr00983

Cannell, M. G. R., & Smith, R. I. (1983). Thermal Time, Chill Days and Prediction of Budburst in Picea sitchensis. *The Journal of Applied Ecology*, *20*(3), 951-963. https://doi.org/10.2307/2403139

Chaffey, N., & Barlow, P. (2002). Myosin, microtubules, and microfilaments: Co-operation between cytoskeletal components during cambial cell division and secondary vascular differentiation in trees. *Planta*, *214*(4), 526–536. https://doi.org/10.1007/s004250100652

Chmielewski, F. M., & Rötzer, T. (2001). Response of tree phenology to climate change across Europe. *Agricultural and Forest Meteorology*, *108*(2), 101–112. https://doi.org/10.1016/S0168-1923(01)00233-7

Chuine, I., Garcia de Cortazar-Atauri, I., Kramer, K., & Hänninen, H. (2013). Plant development models. In M. D. Schwartz (Ed.), *Phenology: an integrative environmental science* (2nd ed., pp. 275–293). Dordrecht: Springer.

Chuine, I., Mignot, A., & Belmonte, J. (2000). A modelling analysis of the genetic variation of phenology between tree populations. *Journal of Ecology*, *88*, 561–570.

Clark, J. S., Salk, C., Melillo, J., & Mohan, J. (2014). Tree phenology responses to winter chilling, spring warming, at north and south range limits. *Functional Ecology*, 28(6), 1344-1355. https://doi.org/10.1111/1365-2435.12309

Coville, F. V. (1920). The Influence of Cold in Stimulating the Growth of Plants. *Proceedings of the National Academy of Sciences of the United States of America*, 434–435. https://doi.org/10.1175/1520-0493(1920)48<643b:TIOCIS>2.0.CO;2

Cuny, H. E., Rathgeber, C. B. K., Lebourgeois, F., Fortin, M., & Fournier, M. (2012). Life strategies in intra-annual dynamics of wood formation: example of three conifer species in a temperate forest in north-east France. *Tree Physiology*, *32*(5), 612–625. https://doi.org/10.1093/treephys/tps039

Delpierre, N., Berveiller, D., Granda, E., & Dufrêne, E. (2016). Wood phenology, not carbon input, controls the interannual variability of wood growth in a temperate oak forest. *New Phytologist*, *210*(2), 459–470. https://doi.org/10.1111/nph.13771

Delpierre, N., Guillemot, J., Dufrêne, E., Cecchini, S., & Nicolas, M. (2017). Tree phenological ranks repeat from year to year and correlate with growth in temperate deciduous forests. *Agricultural and Forest Meteorology*, *234–235*, 1–10. https://doi.org/10.1016/j.agrformet.2016.12.008

Delpierre, N., Soudani, K., François, C., Le Maire, G., Bernhofer, C., Kutsch, W., Misson, L., Rambal, S., Vesala, T., & Dufrêne, E. (2012). Quantifying the influence of climate and biological drivers on the interannual variability of carbon exchanges in European forests through process-based modelling. *Agricultural and Forest Meteorology*, *154–155*, 99–112. https://doi.org/10.1016/j.agrformet.2011.10.010

Delpierre, N., Vitasse, Y., Chuine, I., Guillemot, J., Bazot, S., Rutishauser, T., & Rathgeber, C. B. K. (2016). Temperate and boreal forest tree phenology: from organ-scale processes to terrestrial ecosystem models. *Annals of Forest Science*, *73*(1), 5–25. https://doi.org/10.1007/s13595-015-0477-6

Deslauriers, A., Huang, J.-G., Balducci, L., Beaulieu, M., & Rossi, S. (2016). The Contribution of Carbon and Water in Modulating Wood Formation in Black Spruce Saplings. *Plant Physiology*, *170*(4), 2072–2084. https://doi.org/10.1104/pp.15.01525

Deslauriers, A., Morin, H., & Begin, Y. (2003). Cellular phenology of annual ring formation of Abies balsamea in the Quebec boreal forest (Canada). *Canadian Journal of Forest Research*, *33*(2), 190–200. https://doi.org/10.1139/x02-178

Deslauriers, A., Rossi, S., Anfodillo, T., & Saracino, A. (2008). Cambial phenology, wood formation and temperature thresholds in two contrasting years at high altitude in southern Italy. *Tree Physiology*. https://doi.org/10.1093/treephys/28.6.863

Egierszdorff, S. (1981). The role of auxin stored in scots pine trunk during spring activation of cambial activity. *Biologia Plantarum*, *23*(2), 110–115. https://doi.org/10.1007/BF02878415

Flynn, D. F. B., & Wolkovich, E. M. (2018). Temperature and photoperiod drive spring phenology across all species in a temperate forest community. *New Phytologist*. https://doi.org/10.1111/nph.15232

Ford, K. R., Harrington, C. A., Bansal, S., Gould, P. J., & St. Clair, J. B. (2016). Will changes in phenology track climate change? A study of growth initiation timing in coast Douglas-fir. *Global Change Biology*, *22*(11), 3712–3723. https://doi.org/10.1111/gcb.13328

Fox, J., & Weisberg, S. (2011). *An R companion to applied regression*. *SAGE*. https://doi.org/10.1177/0049124105277200

Fu, Y. H., Campioli, M., Van Oijen, M., Deckmyn, G., & Janssens, I. A. (2012). Bayesian comparison of six different temperature-based budburst models for four temperate tree species. *Ecological Modelling*, *230*, 92–100. https://doi.org/10.1016/j.ecolmodel.2012.01.010

Fu, Y. H., Zhao, H., Piao, S., Peaucelle, M., Peng, S., Zhou, G., Ciais, P., Huang, M., Menzel, A., Peñuelas, J., Song, Y., Vitasse, Y., Zeng, Z., & Janssens, I. A. (2015). Declining global warming effects on the phenology of spring leaf unfolding. *Nature*, *526*(7571), 104–107. https://doi.org/10.1038/nature15402

Gelman, A., Carlin, J. B., Stern, H. S., & Rubin, D. B. (2004). *Bayesian Data Analysis*. *Chapman Texts in Statistical Science Series*. https://doi.org/10.1007/s13398-014-0173-7.2

Gelman, A., Meng, X.-L., & Stern, H. (1996). Posterior predictive assessment of model fitness via realized discrepancies. *Statistica Sinica*, *6*(4), 733–807. https://doi.org/10.1.1.142.9951

Giagli, K., Gricar, J., Vavrcik, H., & Gryc, V. (2016). Nine-year monitoring of cambial seasonality and cell production in Norway spruce, *9*, 375–382. https://doi.org/10.3832/ifor1771-008

Gričar, J., Zupančič, M., Čufar, K., Koch, G., Schmitt, U., & Oven, P. (2006). Effect of local heating and cooling on cambial activity and cell differentiation in the stem of Norway spruce (Picea abies). *Annals of Botany*, *97*(6), 943–951. https://doi.org/10.1093/aob/mcl050

738 Gričar, J., Zupančič, M., Čufar, K., & Oven, P. (2007). Regular cambial activity and xylem and phloem
739 formation in locally heated and cooled stem portions of Norway spruce. *Wood Science and Technology*,
740 *41*(6), 463–475. https://doi.org/10.1007/s00226-006-0109-2

741 Gruber, A., Strobl, S., Veit, B., & Oberhuber, W. (2010). Impact of drought on the temporal dynamics of wood
742 formation in Pinus sylvestris. *Tree Physiology*, *30*(4), 490–501. https://doi.org/10.1093/treephys/tpq003

743 Guillemot, J., Francois, C., Hmimina, G., Dufrêne, E., Martin-StPaul, N. K., Soudani, K., Marie, G., Ourcival,
744 J.-M., & Delpierre, N. (2017). Environmental control of carbon allocation matters for modelling forest
745 growth. *New Phytologist*, *214*(1). https://doi.org/10.1111/nph.14320

746 Hänninen, H. (2016). *Boreal and Temperate Trees in a Changing Climate*. Dordrecht: Springer Netherlands.
747 https://doi.org/10.1007/978-94-017-7549-6

748 Hänninen, H., & Kramer, K. (2007). A Framework for Modelling the Annual Cycle of Trees in Boreal and
749 Temperate. *Silva Fennica*, *41*(1), 167–205.

750 Hartig, F., Minnuno, F., & Paul, S. (2017). BayesianTools: General-Purpose MCMC and SMC Samplers and
751 Tools for Bayesian Statistics. R package version 0.1.5.

752 Heide, O. (1993). Daylength and thermal time responses of budburst during dormancy release in some northern
753 deciduous trees. *Physiologia Plantarum*, *88*(4), 531–540. Retrieved from
754 http://onlinelibrary.wiley.com/doi/10.1111/j.1399-3054.1993.tb01368.x/abstract

755 Huang, J.-G., Deslauriers, A., & Rossi, S. (2014). Xylem formation can be modeled statistically as a function of
756 primary growth and cambium activity. *The New Phytologist*, *203*(3), 831–841.
757 https://doi.org/10.1111/nph.12859

758 Immanen, J., Nieminen, K., Smolander, O. P., Kojima, M., Alonso Serra, J., Koskinen, P., Zhang, J., Elo, A.,
759 Mähönen, A. P., Street, N., Bhalerao, R. P., Paulin, L., Auvinen, P., Sakakibara, H., & Helariutta, Y.
760 (2016). Cytokinin and Auxin Display Distinct but Interconnected Distribution and Signaling Profiles to
761 Stimulate Cambial Activity. *Current Biology*, *26*(15), 1990–1997.
762 https://doi.org/10.1016/j.cub.2016.05.053

763 Jyske, T., Mäkinen, H., Kalliokoski, T., & Nöjd, P. (2014). Intra-annual tracheid production of Norway spruce
764 and Scots pine across a latitudinal gradient in Finland. *Agricultural and Forest Meteorology*, *194*, 241–
765 254. https://doi.org/10.1016/j.agrformet.2014.04.015

766 Kass, R. E., & Raftery, A. E. (1995). Bayes factors. *Journal of the American Statistical Association*, *90*(430),
767 773–795. https://doi.org/10.1080/01621459.1995.10476572

768 Kramer, K. (1995). Modelling comparison to evaluate the importance of phenology for the effects of climate
769 change on growth of temperate-zone deciduous trees. *Climate Research*, *5*, 119–130.

770 Larson, P. (1994). *The vascular cambium: development and structure. Springer*. https://doi.org/10.1007/978-3-

642-78466-8

Lempereur, M., Martin-stpaul, N. K., Damesin, C., Joffre, R., Ourcival, J., Rocheteau, A., & Rambal, S. (2015). Growth duration is a better predictor of stem increment than carbon supply in a Mediterranean oak forest : implications for assessing forest productivity under climate change. *New Phytologist*, *207*, 579–590.

Li, X., Liang, E., Gričar, J., Rossi, S., Čufar, K., & Ellison, A. M. (2017). Critical minimum temperature limits xylogenesis and maintains treelines on the southeastern Tibetan Plateau. *Science Bulletin*, *62*(11), 804–812. https://doi.org/10.1016/j.scib.2017.04.025

Linkosalo, T., Carter, T. R., Hakkinen, R., & Hari, P. (2000). Predicting spring phenology and frost damage risk of Betula spp. under climatic warming: A comparison of two models. *Tree Physiology*, *20*(17), 1175–1182. https://doi.org/10.1093/treephys/20.17.1175

Little, C. H. A., & Bonga, J. M. (1974). Rest in the cambium of Abies balsamea. *Canadian Journal of Botany*, *52*, 1723–1730.

Lupi, C., Morin, H., Deslauriers, A., & Rossi, S. (2010). Xylem phenology and wood production: resolving the chicken-or-egg dilemma. *Plant, Cell & Environment*, *33*(10), 1721–1730. https://doi.org/10.1111/j.1365-3040.2010.02176.x

Mäkelä, A., Hari, P., Berninger, F., Hänninen, H., & Nikinmaa, E. (2004). Acclimation of photosynthetic capacity in Scots pine to the annual cycle of temperature. *Tree Physiology*, *24*(4), 369–376. https://doi.org/10.1093/treephys/24.4.369

Mäkinen, H., Jyske, T., & Nöjd, P. (2018). Dynamics of diameter and height increment of Norway spruce and Scots pine in southern Finland. *Annals of Forest Science*, *75*(1): 28. https://doi.org/10.1007/s13595-018-0710-1

Mesplé, F., Troussellier, M., Casellas, C., & Legendre, P. (1996). Evaluation of simple statistical criteria to qualify a simulation. *Ecological Modelling, 88,* 9-18. https://doi.org/10.1016/0304-3800(95)00033-X

Michelot, A., Simard, S., Rathgeber, C., Dufrêne, E., & Damesin, C. (2012). Comparing the intra-annual wood formation of three European species (Fagus sylvatica, Quercus petraea and Pinus sylvestris) as related to leaf phenology and non-structural carbohydrate dynamics. *Tree Physiology*, *32*(8), 1033–1045. https://doi.org/10.1093/treephys/tps052

Moser, L., Fonti, P., Büntgen, U., Esper, J., Luterbacher, J., Franzen, J., & Frank, D. (2010). Timing and duration of European larch growing season along altitudinal gradients in the Swiss Alps. *Tree Physiology*, *30*(2), 225–233. https://doi.org/10.1093/treephys/tpp108

O'Hagan, A. (1995). Fractional Bayes Factors for Model Comparison. *Journal of the Royal Statistical Society: Series B (Methodological)*, *57*(1), 99–138. https://doi.org/10.2307/2346088

Olsson, C., & Jönsson, A. M. (2014). Process-based models not always better than empirical models for

simulating budburst of Norway spruce and birch in Europe. *Global Change Biology*, *20*(11), 3492–3507. https://doi.org/10.1111/gcb.12593

Oribe, Y., Funada, R., & Kubo, T. (2003). Relationships between cambial activity , cell differentiation and the localization of starch in storage tissues around the cambium in locally heated stems of Abies sachalinensis (Schmidt) Masters. *Trees*, *17*, 185–192. https://doi.org/10.1007/s00468-002-0231-1

Oribe, Y., & Kubo, T. (1997). Effect of heat on cambial reactivation during winter dormancy in evergreen and deciduous conifers. *Tree Physiology*, *17*(2), 81–87. https://doi.org/10.1093/treephys/17.2.81

Osada, N., Murase, K., Tsuji, K., Sawada, H., Nunokawa, K., Tsukahara, M., & Hiura, T. (2018). Genetic differentiation in the timing of budburst in Fagus crenata in relation to temperature and photoperiod. *International Journal of Biometeorology*, 1–14. https://doi.org/10.1007/s00484-018-1579-2

Pelkonen, P., & Hari, P. (1980). The dependence of the springtime recovery of CO_2 uptake in Scots pine on temperature and internal factors. *Flora*, *169*, 398–404. Retrieved from citeulike-article-id:7556840

Perrin, M., Rossi, S., & Isabel, N. (2017). Synchronisms between bud and cambium phenology in black spruce: Early-flushing provenances exhibit early xylem formation. *Tree Physiology*, *37*(5), 593–603. https://doi.org/10.1093/treephys/tpx019

Petterle, A., Karlberg, A., & Bhalerao, R. P. (2013). Daylength mediated control of seasonal growth patterns in perennial trees. *Current Opinion in Plant Biology*. https://doi.org/10.1016/j.pbi.2013.02.006

Piñeiro, G., Perelman, S., Guerschman, J. P., & Paruelo, J. M. (2008). How to evaluate models: Observed vs. predicted or predicted vs. observed? *Ecological Modelling*, *216*(3–4), 316–322. https://doi.org/10.1016/j.ecolmodel.2008.05.006

Prislan, P., Čufar, K., Koch, G., Schmitt, U., & Gričar, J. (2013). Review of cellular and subcellular changes in the cambium. *IAWA Journal*, *34*(4), 391–407. https://doi.org/10.1163/22941932-00000032

Prislan, P., Schmitt, U., Koch, G., Gričar, J., & Čufar, K. (2011). Seasonal ultrastructural changes in the cambial zone of beech (Fagus Sylvatica) grown at two different altitudes. *IAWA Journal*, *32*(4), 443–459.

Rathgeber, C. B. K., Longuetaud, F., Mothe, F., Cuny, H., & Le Moguédec, G. (2011). Phenology of wood formation: Data processing, analysis and visualisation using R (package CAVIAR). *Dendrochronologia*, *29*(3), 139–149. https://doi.org/10.1016/j.dendro.2011.01.004

Rensing, K. H., & Samuels, a. L. (2004). Cellular changes associated with rest and quiescence in winter-dormant vascular cambium of Pinus contorta. *Trees*, *18*(4), 373–380. https://doi.org/10.1007/s00468-003-0314-7

Rinne, P. L. H., Kaikuranta, P. M., Van Der Schoot, C., Schoot, C. Van Der, Conservation, N., & Physiology, P. D. (2001). The shoot apical meristem restores its symplasmic organization during chilling-induced release from dormancy. *The Plant Journal*, *26*(3), 249–264. https://doi.org/10.1046/j.1365-313X.2001.01022.x

837 Rossi, S., Anfodillo, T., Čufar, K., Cuny, H. E., Deslauriers, A., Fonti, P., Frank, D., Gričar, J., Gruber, A.,
838 Huang, J.-G., Jyske, T., Kaspar, J., King, G., Krause, C., Liang, E., Mäkinen, H., Morin, H., Nöjd, P.,
839 Oberhuber, W., Prislan, P., Rathgeber, C.B.K., Saracino, A., Swidrak, I., & Treml, V. (2016). Pattern of
840 xylem phenology in conifers of cold ecosystems at the Northern Hemisphere. *Global Change Biology*,
841 *22*(11), 3804–3813. https://doi.org/10.1111/gcb.13317

842 Rossi, S., Anfodillo, T., & Menardi, R. (2006). TREPHOR: a new tool for sampling microcores from tree stems.
843 *IAWA Journal*, *27*(1), 89–97.

844 Rossi, S., Deslauriers, A., & Anfodillo, T. (2006). Assessment of cambial activity and xylogenesis by
845 microsampling tree species: An example at the Alpine timberline. *IAWA Journal*.
846 https://doi.org/10.1163/22941932-90000161

847 Rossi, S., Deslauriers, A., Anfodillo, T., & Carraro, V. (2007). Evidence of threshold temperatures for
848 xylogenesis in conifers at high altitudes. *Oecologia*, *152*(1), 1–12. https://doi.org/10.1007/s00442-006-
849 0625-7

850 Rossi, S., Deslauriers, A., Griçar, J., Seo, J.-W., Rathgeber, C. B. K., Anfodillo, T., Morin, H., Levanic, T.,
851 Oven, P., & Jalkanen, R. (2008). Critical temperatures for xylogenesis in conifers of cold climates. *Global*
852 *Ecology and Biogeography*, *17*(6), 696–707. https://doi.org/10.1111/j.1466-8238.2008.00417.x

853 Rossi, S., Morin, H., Deslauriers, A., & Plourde, P.-Y. (2011). Predicting xylem phenology in black spruce under
854 climate warming. *Global Change Biology*, *17*(1), 614–625. https://doi.org/10.1111/j.1365-
855 2486.2010.02191.x

856 Rossi, S., Rathgeber, C. B. K., Deslauriers, A., Sergio, R., Cyrille, B. K. R., & Annie, D. (2009). Comparing
857 needle and shoot phenology with xylem development on three conifer species in Italy. *Annals of Forest*
858 *Science*, *66*(2), 1–8.

859 Sakai, A. (1966). Studies of Frost Hardiness in Woody Plants. II. Effect of Temperature on Hardening. *Plant*
860 *Physiology*, *41*(2), 353–359. https://doi.org/10.1104/pp.41.2.353

861 Sakai, A., & Larcher, W. (1987). *Frost survival of plants: responses and adaptation to freezing stress*.
862 *Ecological studies*. https://doi.org/10.1007/BF02854542

863 Sarvas, R. (1974). *Investigations on the annual cycle of development of forest trees. II. Autumn dormancy and*
864 *winter dormancy*. *Communicationes Instituti Forestalis Fenniae*.

865 Schaller, G. E., Street, I. H., & Kieber, J. J. (2014). Cytokinin and the cell cycle. *Current Opinion in Plant*
866 *Biology*, *21*, 7–15. https://doi.org/10.1016/j.pbi.2014.05.015

867 Schiestl-Aalto, P., Kulmala, L., Mäkinen, H., Nikinmaa, E., & Mäkelä, A. (2015). CASSIA - a dynamic model
868 for predicting intra-annual sink demand and interannual growth variation in Scots pine. *New Phytologist*,
869 *206*(2), 647–659. https://doi.org/10.1111/nph.13275

Schmitt, U., Jalkanen, R., & Eckstein, D. (2004). Cambium dynamics of Pinus sylvestris and Betula spp. in the northern boreal forest in Finland. *Silva Fennica*, *38*(2), 167–178. https://doi.org/10.14214/sf.426

Seo, J.-W. J., Eckstein, D., Jalkanen, R., Rickebusch, S., & Schmitt, U. W. E. (2008). Estimating the onset of cambial activity in Scots pine in northern Finland by means of the heat-sum approach. *Tree Physiology*, *28*(1), 105–112. https://doi.org/10.1093/treephys/28.1.105

Singh, R. K., Svystun, T., AlDahmash, B., Jönsson, A. M., & Bhalerao, R. P. (2017). Photoperiod- and temperature-mediated control of phenology in trees – a molecular perspective. *New Phytologist*. https://doi.org/10.1111/nph.14346

Sorce, C., Giovannelli, A., Sebastiani, L., & Anfodillo, T. (2013). Hormonal signals involved in the regulation of cambial activity, xylogenesis and vessel patterning in trees. *Plant Cell Reports*, *32*(6), 885–898. https://doi.org/10.1007/s00299-013-1431-4

Strimbeck, G. R., Schaberg, P. G., Fossdal, C. G., Schröder, W. P., & Kjellsen, T. D. (2015). Extreme low temperature tolerance in woody plants. *Frontiers in Plant Science*, *6*, 884. https://doi.org/10.3389/fpls.2015.00884

Swidrak, I., Gruber, A., Kofler, W., & Oberhuber, W. (2011). Effects of environmental conditions on onset of xylem growth in Pinus sylvestris under drought. *Tree Physiology*, *31*(5), 483–493. https://doi.org/10.1093/treephys/tpr034

Takahashi, S., Okada, N., & Nobuchi, T. (2013). Relationship between the timing of vessel formation and leaf phenology in ten ring-porous and diffuse-porous deciduous tree species. *Ecological Research*, *28*(4), 615–624. https://doi.org/10.1007/s11284-013-1053-x

Vaganov, E. A., Hughes, M. K., & Shashkin, A. V. (2006). *Growth Dynamics of Conifer Tree Rings: Images of Past and Future Environments* . *Springer* (Vol. 83). https://doi.org/10.1007/3-540-31298-6

van Oijen, M., Reyer, C., Bohn, F. J., Cameron, D. R., Deckmyn, G., Flechsig, M., Härkönen, S., Hartig., F., Huth, A., Kiviste, A., Lasch, P., Mäkelä, A., Mette, T., Minnuno, F., & Rammer, W. (2013). Bayesian calibration, comparison and averaging of six forest models, using data from Scots pine stands across Europe. *Forest Ecology and Management*, *289*, 255–268. https://doi.org/10.1016/j.foreco.2012.09.043

Verdier, B., Jouanneau, I., Simonnet, B., Rabin, C., Van Dooren, T. J. M., Delpierre, N., Clobert, J., Abbadie, L., Ferrière, R., & Le Galliard, J. F. (2014). Climate and atmosphere simulator for experiments on ecological systems in changing environments. *Environmental Science and Technology*, *48*(15), 8744–8753. https://doi.org/10.1021/es405467s

Vitasse, Y., Delzon, S., Bresson, C. C., Michalet, R., & Kremer, A. (2009). Altitudinal differentiation in growth and phenology among populations of temperate-zone tree species growing in a common garden. *Canadian Journal of Forest Research*, *39*(7), 1259–1269. https://doi.org/10.1139/X09-054

Vitasse, Y., François, C., Delpierre, N., Dufrêne, E., Kremer, A., Chuine, I., & Delzon, S. (2011). Assessing the

effects of climate change on the phenology of European temperate trees. *Agricultural and Forest Meteorology*, *151*(7), 969–980. https://doi.org/10.1016/j.agrformet.2011.03.003

von Wuehlisch, G., Krusche, D., & Muhs, H. J. (1995). Variation in temperature sum requirement for flushing of beech provenances. *Silvae Genetica, 44 (5-6)*, 343-346.

Weedon, G. P., Balsamo, G., Bellouin, N., Gomes, S., Best, M. J., & Viterbo, P. (2014). The WFDEI meteorological forcing data set: WATCH Forcing Data methodology applied to ERA-Interim reanalysis data. *Water Resources Research*, *50*(9), 7505–7514. https://doi.org/10.1002/2014WR015638

Tables

Table 1. Overview of the tested models and their parameters. T_a= daily average air temperature (°C); *DL*= photoperiod (hours). See text for definition of the model parameters.

Model name	Type	Environmental variables	Fitted parameters (number)	Equation reference
Tt	temperature *threshold*	T_a	T* (1)	1
TDLt	temperature and photoperiod *thresholds*	T_a, DL	DL*, T* (2)	2
HS	*Heat sum*	T_a, DL	DLF_{start}, T_f, F* (3)	3-5
CiHS	*Chilling-influenced heat sum*	T_a, DL	DLC_{start}, DLC_{end}, DLF_{start}, T_c, T_f, g, h (7)	6-8
MST	Regression line	January-June average temperature	mT_{spg}, pT_{spg} (2)	9

Table 2. Overview of the wood phenology data. bE= date of the beginning of xylem cell enlargement (DoY), ΔbE= amplitude of bE dates (days). The 'within site-year SD' metric is the average standard deviation of bE among trees sampled on a given site-year.

Tree species	Number of site-years	Number of observations	Mean bE (DoY)	SD of bE (days)	Min. bE (DoY)	Max. bE (DoY)	ΔbE within-species (days)	Within-site-year SD (days)
LADE	62	300	150	12	118	183	65	5.4
PISY	37	175	112	20	75	176	101	5.4
PCAB	77	336	136	16	101	177	76	4.2
PCMA	42	294	152	9	128	177	49	4.8

Table 3. Model performance comparison. PMW= posterior model weight (eq. 11); RMSE= root mean square error (days); ΔAICc= differential Akaike Information Criterion, corrected for small sample biases (calculated as the difference from minimum AICc across all models; according to this metric, the best model at maximum likelihood has a score of 0). PMWs are established over the whole posterior distribution. RMSE and AICc were calculated at the point of maximum likelihood (MAP). We report here the medians of those metrics, established across the 30 calibration re-samplings. The *CiHS* model results appear in bold characters, as displaying the highest PMW over validation data in all species.

	Model class	Model name	PMW_{calib}	PMW_{valid}	$RMSE_{calib}$	$RMSE_{valid}$	$\Delta AICc_{calib}$	$\Delta AICc_{valid}$
LADE (n calib= 210, n valid=90)	threshold	Tt	0.00	0.00	14.7	15.0	226	89
	threshold	TDLt	0.00	0.00	9.9	10.3	95	30
	heat sum	HS	0.00	0.01	8.2	8.7	36	8
	chilling-influenced heat sum	**CiHS**	**1.00**	**0.94**	**7.5**	**8.1**	**0**	**0**
	regression	MST	0.00	0.00	8.7	8.9	53	13
PISY (n calib = 123, n valid = 52)	threshold	Tt	0.00	0.00	21.5	24.6	208	98
	threshold	TDLt	0.00	0.00	14.6	15.2	119	46
	heat sum	HS	0.00	0.00	11.4	11.2	63	18
	chilling-influenced heat sum	**CiHS**	**1.00**	**1.00**	**8.4**	**9.3**	**0**	**0**

	regression	MST	0.00	0.00	15.6	15.6	133	49
PCAB (n calib = 236, n valid = 100)	threshold	Tt	0.00	0.00	16.8	17.2	378	151
	threshold	TDLt	0.00	0.00	12.4	12.6	221	92
	heat sum	HS	0.00	0.00	9.8	10.1	119	35
	chilling-influenced heat sum	**CiHS**	**1.00**	**1.00**	**7.5**	**7.9**	**0**	**0**
	regression	MST	0.00	0.00	11.5	11.6	154	62
PCMA (n calib = 206, n valid = 88)	threshold	Tt	0.00	0.00	13.1	13.2	334	139
	threshold	TDLt	0.00	0.00	7.3	7.3	116	45
	heat sum	HS	0.00	0.00	5.8	6.1	38	15
	chilling-influenced heat sum	**CiHS**	**1.00**	**0.67**	**5.2**	**5.6**	**0**	**0**
	regression	MST	0.00	0.33	6.7	6.9	32	1

925

Table 4. Assessment of model bias on validation data. We tested the model ability to produced unbiased predictions of bE from the validation subsets at different scales, with two different methods (see Material and Methods 2.6 for details). The slopes and intercepts estimates are reported with their 95%-confidence intervals between parentheses. Unbiased predictions are characterized by both slope= 1 and intercept=0. In Method 1, we report the p-value of the Wald test (testing for unit slope and zero intercept as the null hypothesis). In Method 2, we identify biased predictions when either the slope or intercept confidence intervals do not include one or zero, respectively. 'yes' / 'no' mark biased / unbiased predictions.

		Method 1					Method 2		
bE data aggregation scale	Species	slope	intercept	F	P(>F)	Bias ?	slope	intercept	Bias ?
tree	LADE	1.04 (0.93, 1.15)	-6.2 (-23.0, 10.6)	0.41	0.66	**no**	0.67 (0.60, 0.74)	49.6 (38.4, 60.0)	yes
	PISY	1.02 (0.91, 1.12)	-4.2 (-16.5, 8.1)	2.57	0.08	**no**	0.79 (0.71, 0.87)	25.9 (16.3, 34.8)	yes
	PCAB	0.98 (0.92, 1.04)	2.5 (-5.4, 10.4)	0.34	0.71	**no**	0.88 (0.83, 0.93)	16.1 (8.9, 22.9)	yes
	PCMA	1.04 (0.94, 1.15)	-7.2 (-23.2, 8.7)	1.31	0.27	**no**	0.68 (0.61, 0.75)	49.2 (38.5, 59.2)	yes
site-year*	LADE	1.06 (0.90, 1.22)	-9.4 (-33.5, 14.6)	0.34	0.71	**no**	0.80 (0.68, 0.92)	30.6 (11.52, 47.6)	yes
	PISY	1.02 (0.85, 1.19)	-4.1 (-24.4, 16.2)	0.84	0.44	**no**	0.88 (0.74, 1.04)	15.4 (-3.1, 31.4)	**no**
	PCAB	0.99 (0.88, 1.10)	2.2 (-12.7, 17.1)	0.19	0.83	**no**	0.91 (0.81, 1.02)	11.8 (-2.6, 24.9)	**no**
	PCMA	1.01 (0.87, 1.16)	-3.1 (-25.1, 19.0)	1.83	0.18	**no**	0.91 (0.79, 1.05)	14.5 (-6.2, 33.3)	**no**
site*	LADE	1.13 (0.87, 1.40)	-19.3 (-58.8, 20.2)	0.72	0.51	**no**	0.82 (0.65, 1.04)	25.9 (-6.1, 52.3)	**no**
	PISY	1.03 (0.82, 1.23)	-6.0 (-31.3, 19.2)	0.97	0.4	**no**	0.92 (0.75, 1.13)	11.7 (-12.5, 31.8)	**no**
	PCAB	1.01 (0.83, 1.20)	-1.8 (-26.6, 23.1)	0.02	0.98	**no**	0.91 (0.76, 1.09)	11.47 (-13.0,	**no**

								32.2)	
	PCMA	1.27 (0.86, 1.68)	-42.0 (-102.1, 18.2)	3.55	0.11	**no**	0.75 (0.53, 1.03)	38.4 (-1.8, 70.2)	**no**
year anomaly**	LADE	1.02 (0.81, 1.23)	0 (-1.1, 1.1)	0.02	0.98	**no**	0.73 (0.59, 0.89)	0 (0, 0)	yes
	PISY	1.20 (0.67, 1.74)	0 (-2.0, 2.0)	0.3	0.74	**no**	0.43 (0.25, 0.64)	0 (0, 0)	yes
	PCAB	1.17 (1.00, 1.34)	0 (-1.1, 1.1)	2.02	0.14	**no**	0.69 (0.60, 0.80)	0 (0, 0)	yes
	PCMA	0.89 (0.74, 1.04)	0 (-0.8, 0.8)	1.06	0.36	**no**	1.02 (0.86, 1.21)	0 (0, 0)	**no**

* bE dates were simulated at the tree individual scale, and subsequently averaged at the site-year or site scale; ** bE dates were simulated at the tree individual scale. For calculating annual anomalies, we subtracted the average bE date, established along the observation period, to bE data averaged at the site-year scale.

Figure captions

Figure 1. Location of the study sites.

Figure 2. Climate space at the observed date of bE. Each bE datum is placed in a climate space defined by the day length at bE (x-axis) and the average temperature over the 15-day interval preceding bE (y-axis).

Figure 3. Chilling-influenced heat sum (*CiHS*) model evaluation over validation data. Predictions are reported at the tree scale (grey dots) and aggregated site-year scale (points, colours according to the average January-June temperature of the site-year). The thick black line is the least square regression line of predicted versus observed data. The one-to-one relation appears as the thin grey line. *NSE*= Nash-Sutcliffe model efficiency; *slope*= slope of the linear regression; *int*= intercept of the linear regression. The displayed statistics are calculated for site-year aggregated data. See Table 3 for statistics on tree-scale data.

Figure 4. Posterior parameter distributions. Parameters are shown for the *CiHS* model, which performed best over the validation data for each species. Grey lines represent each of the 30 inference procedures, with the overall distribution appearing as coloured line. For each parameter, the limits on the x-axis mark the bounds set to the uniform prior density. The mode of the overall distribution appears for each parameter on the upper left-hand corner (e.g. DL_{Cstart} = 12.7 hours for LADE). See Material and Methods for parameters description, and Table S2 for parameter values at the mode of the merged 30 posterior distributions.

Figure 5. Variations of chilling and forcing accumulation time intervals along latitudinal gradients. This figure displays the temporal interval of chilling accumulation (with the starting date plotted as '*' and the ending date as 'o', linked by a straight line) and the starting date of forcing (plotted as '△'). The colour of the symbols indicates the northernmost (blue) or southernmost (red) latitude by species. For PCAB, we also illustrate an intermediate situation (latitude = 54°N, grey symbols). Dashed black line represents vernal equinox; continuous black line represents summer solstice.

Figure 6. Comparing observed and simulated interspecific differences in the date of bE. For those site-years where two species of interest have been sampled simultaneously, we plotted the observed and predicted between-species differences in bE dates (ΔbE, days). Each

964 single point represents one site-year. (a, b): compare the distribution of differences; (c, d):
965 compare observed and predicted differences for each site-year.

Supporting information

Additional supporting information may be found in the online version of this article.

Figure S1. Logistic models are precise in determining temperature thresholds for the beginning of xylem growth, but are not predictive.

Figure S2. Model evaluation performance over validation data, aggregated per site.

Figure S3. Model evaluation performance over validation data, for annual anomalies.

Table S1. Study sites.

Table S2. Parameter values for the chilling-influenced heat sum (*CiHS*) model.

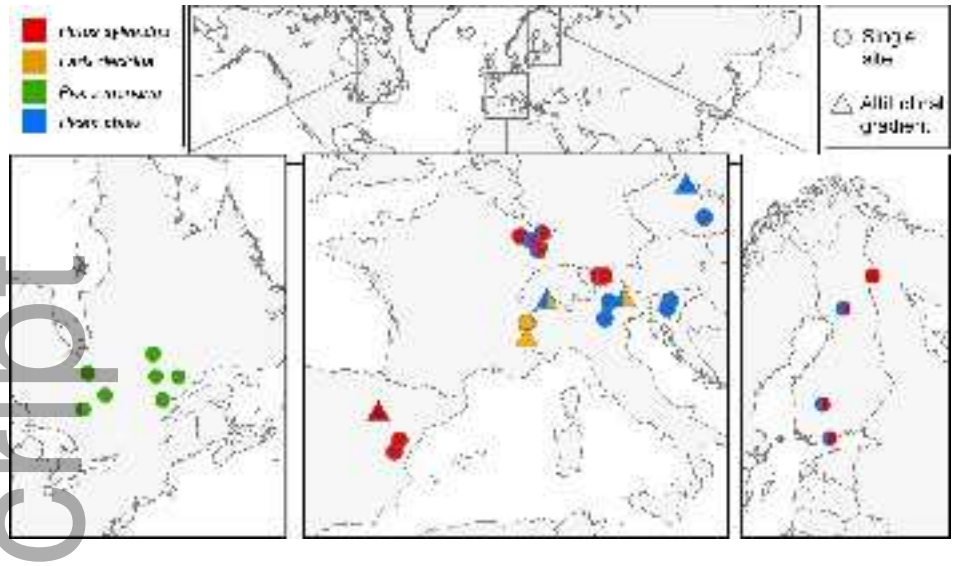

gcb_14539_f1.tif

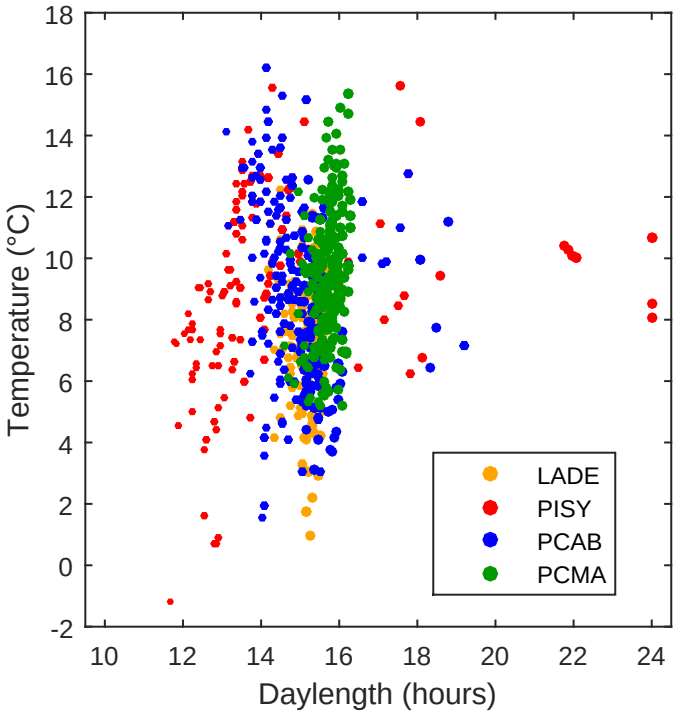

gcb_14539_f2.eps

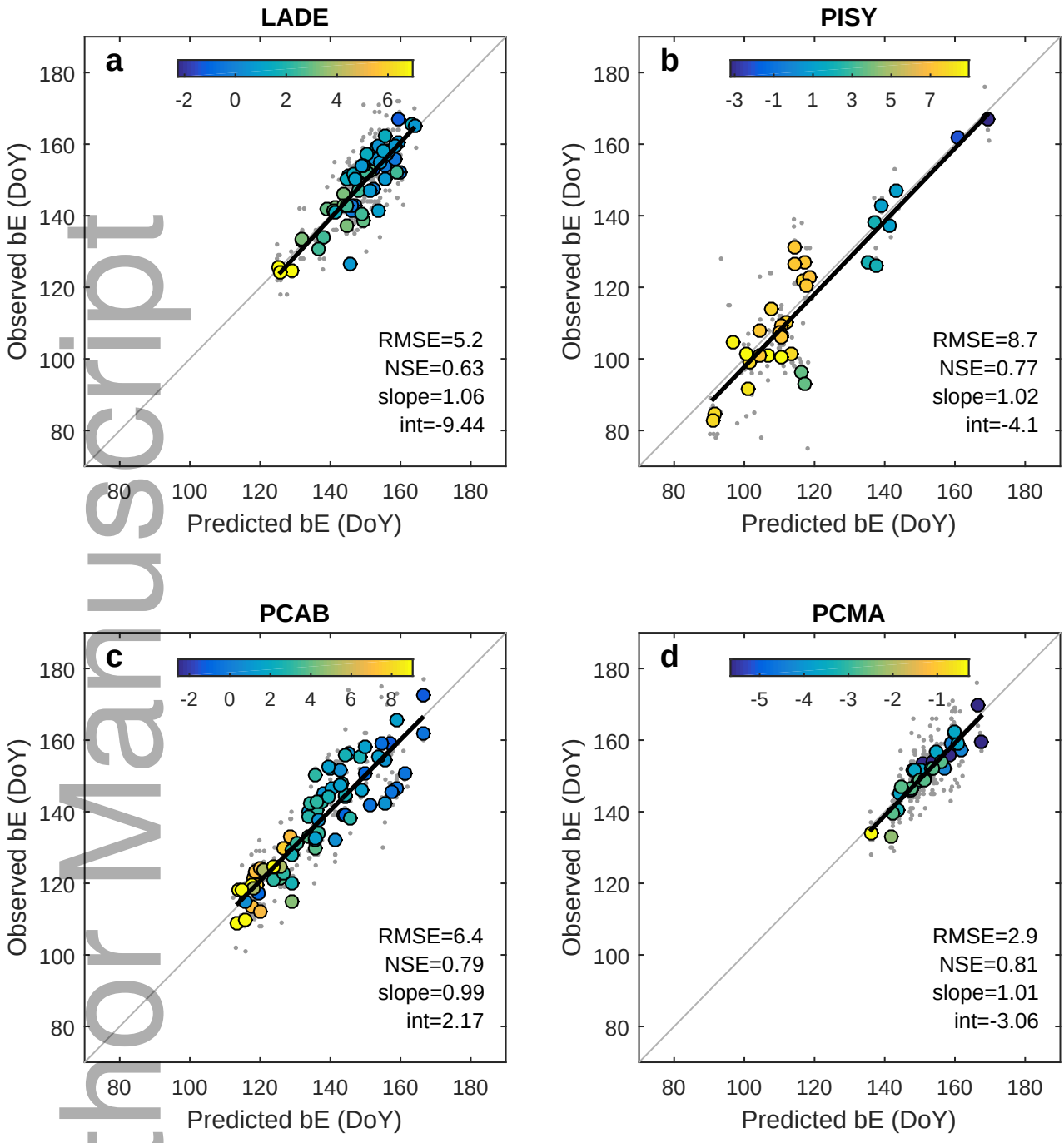

gcb_14539_f3.eps

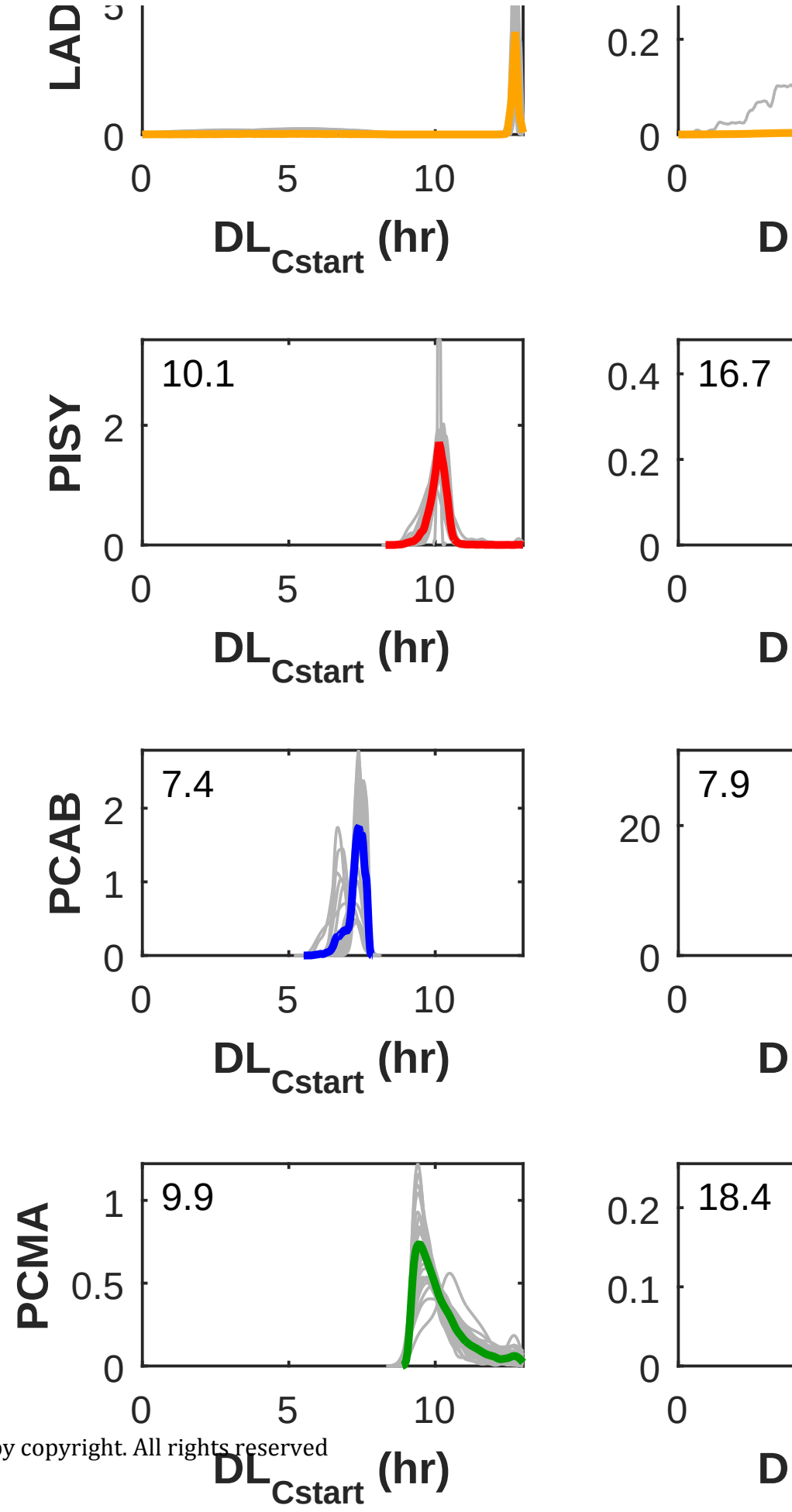

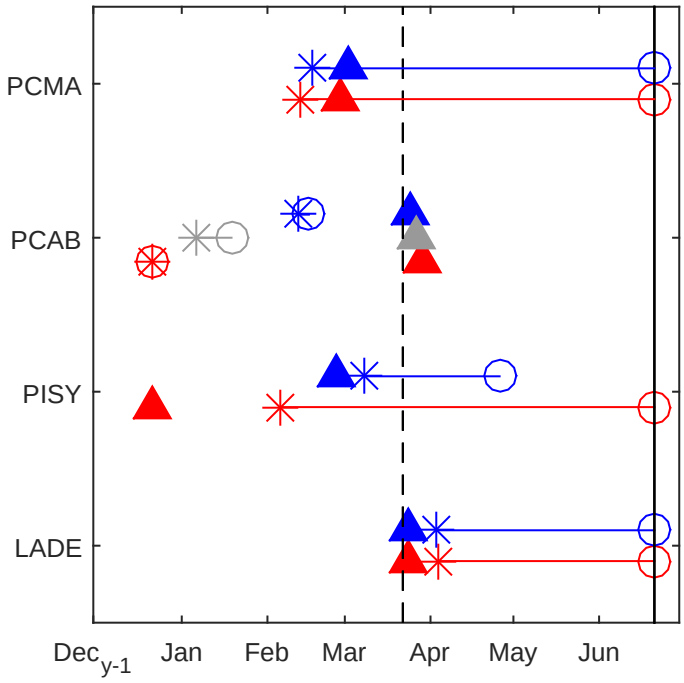

gcb_14539_f5.eps

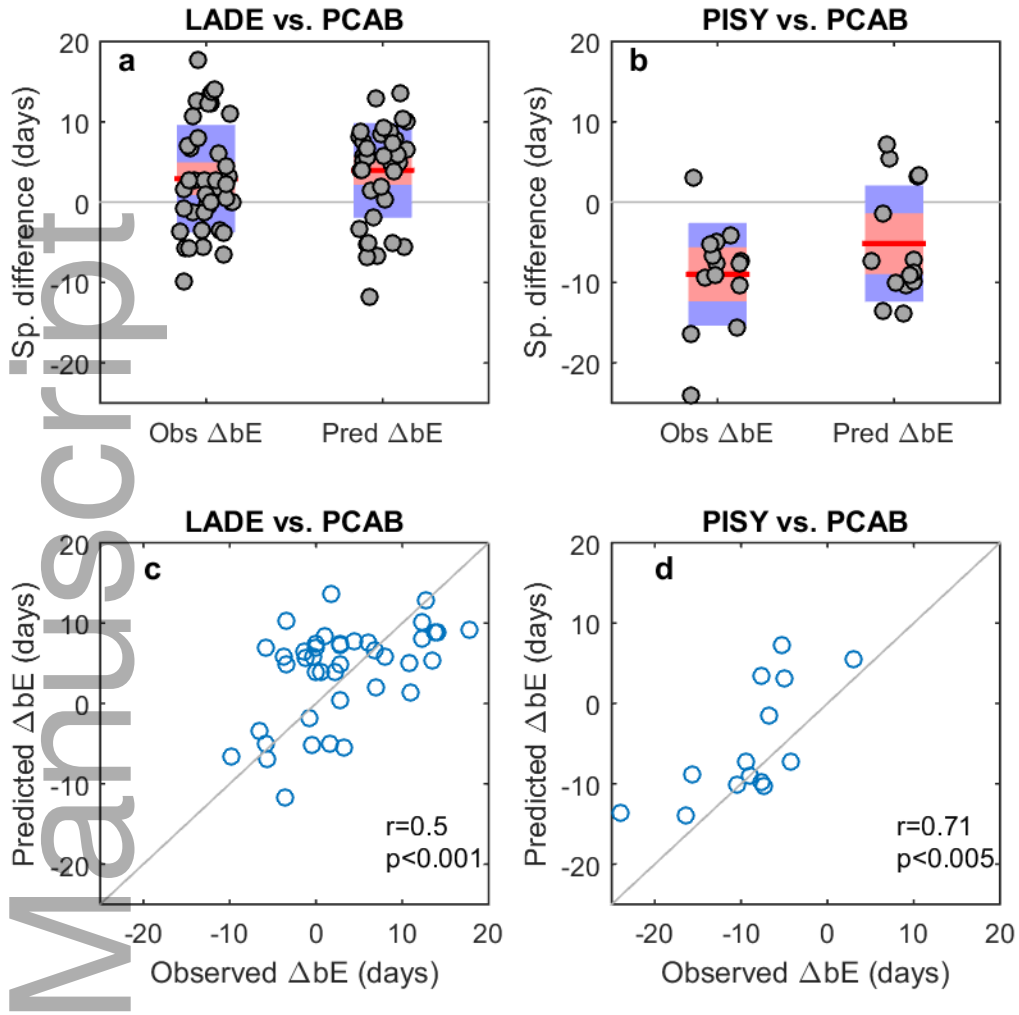

gcb_14539_f6.tif